Photosynth Res
DOI 10.1007/s11120-016-0281-7

ORIGINAL ARTICLE

Influence of light and nitrogen on the photosynthetic efficiency in the C_4 plant *Miscanthus* × *giganteus*

Jian-Ying Ma[1,2] · Wei Sun[2,3] · Nuria K. Koteyeva[4] · Elena Voznesenskaya[4] · Samantha S. Stutz[2] · Anthony Gandin[2] · Andreia M. Smith-Moritz[5] · Joshua L. Heazlewood[5,6] · Asaph B. Cousins[2]

Received: 5 August 2015 / Accepted: 26 May 2016

Abstract There are numerous studies describing how growth conditions influence the efficiency of C_4 photosynthesis. However, it remains unclear how changes in the biochemical capacity versus leaf anatomy drives this acclimation. Therefore, the aim of this study was to determine how growth light and nitrogen availability influence leaf anatomy, biochemistry and the efficiency of the CO_2 concentrating mechanism in *Miscanthus* × *giganteus*. There was an increase in the mesophyll cell wall surface area but not cell well thickness in the high-light (HL) compared to the low-light (LL) grown plants suggesting a higher mesophyll conductance in the HL plants, which also had greater photosynthetic capacity. Additionally, the HL plants had greater surface area and thickness of bundle-sheath cell walls compared to LL plants, suggesting limited differences in bundle-sheath CO_2 conductance because the increased area was offset by thicker cell walls. The gas exchange estimates of phospho*enol*pyruvate carboxylase (PEPc) activity were significantly less than the in vitro PEPc activity, suggesting limited substrate availability in the leaf due to low mesophyll CO_2 conductance. Finally, leakiness was similar across all growth conditions and generally did not change under the different measurement light conditions. However, differences in the stable isotope composition of leaf material did not correlate with leakiness indicating that dry matter isotope measurements are not a good proxy for leakiness. Taken together, these data suggest that the CO_2 concentrating mechanism in Miscanthus is robust under low-light and limited nitrogen growth conditions, and that the observed changes in leaf anatomy and biochemistry likely help to maintain this efficiency.

Keywords Carbon isotope discrimination · C_4 photosynthesis · Miscanthus · Nitrogen · Light

Electronic supplementary material The online version of this article (doi:10.1007/s11120-016-0281-7) contains supplementary material, which is available to authorized users.

✉ Asaph B. Cousins
acousin@wsu.edu

1 Key Laboratory of Biogeography and Bioresource in Arid Land, Xinjiang Institute of Ecology and Geography, Chinese Academy of Sciences, Urumqi 830011, China

2 School of Biological Science, Washington State University, Pullman, WA 99163, USA

3 Institute of Grassland Science, Key Laboratory of Vegetation Ecology, Ministry of Education, Northeast Normal University, Changchun 130024, China

4 Laboratory of Anatomy and Morphology, V.L. Komarov Botanical Institute of the Russian Academy of Sciences, St. Petersburg, Russia

5 Joint BioEnergy Institute and Physical Biosciences Division, Lawrence Berkeley National Laboratory, Berkeley, CA 94720, USA

6 ARC Centre of Excellence in Plant Cell Walls, School of BioSciences, The University of Melbourne, Melbourne, VIC 3010, Australia

Introduction

The CO_2 concentrating mechanism in C_4 plants generally allows for high rates of net CO_2 assimilation and biomass production. During C_4 photosynthesis, bicarbonate (HCO_3^-) is used to carboxylate phospho*enol*pyruvate (PEP) in the mesophyll cells by PEP-carboxylase (PEPc) (Hatch et al. 1967). This reaction generates four-carbon acids, which are subsequently decarboxylated in bundle-sheath cells where ribulose-1,5-bisphosphate carboxylase/

Published online: 16 August 2016

oxygenase (Rubisco) and the majority of the C_3 cycle is compartmentalized. The CO_2 concentrated around Rubisco is typically sufficient to minimize rates of photorespiration; however, the efficiency of this CO_2 concentrating mechanism is influenced by the balance between rates of PEPc carboxylation (v_p) and Rubisco carboxylation (v_c), and the conductance of CO_2 between the bundle-sheath and mesophyll cells (g_{bs}). Unfortunately, the efficiency of the CO_2 concentrating mechanism is not directly measurable; however, leakiness (ϕ), defined as the fraction of CO_2 that is pumped into the bundle-sheath cells that subsequently leaks back out, is often used as a proxy (Farquhar 1983; Hatch et al. 1995).

There have been a number of studies describing how changes in growth conditions (e.g. light, CO_2 concentrations, nitrogen, salinity, drought) influence the efficiency of photosynthesis in a variety of C_4 species. For example, leakiness was minimal in low-light grown *Zea mays*, *Flaveria bidentis, Bienertia sinuspersici* and tended to be lower than high-light grown plants when measured under low photon flux density (PFD) (Kromdijk et al. 2010; Pengelly et al. 2010; Bellasio and Griffiths 2014a, b; Stutz et al. 2014). However, in *Amaranthus cruentus*, the analysis of leaf stable isotope compositions ($\delta^{13}C$) suggested that the efficiency of C_4 photosynthesis was not able to acclimate to the low-light conditions (Tazoe et al. 2006). Additionally, early direct measurements of leaf CO_2 isotope exchange ($\Delta^{13}C$) also indicated that leakiness increased under low PFD measurement (Tazoe et al. 2008; Cousins et al. 2008). However, as discussed below, there are questions regarding the use of $\Delta^{13}C$ to estimate the efficiency of C_4 photosynthesis. Additionally, inaccurate parameterization of bundle-sheath CO_2 concentrations and rates of respiration can artificially increase estimates of leakiness using direct measures of $\Delta^{13}C$ (Ubierna et al. 2011, 2013; Kromdijk et al. 2014). These recent publications comparing direct measurements of $\Delta^{13}C$ and complete models of leaf CO_2 isotope exchange suggest that C_4 photosynthesis can acclimate to growth under low light to maintain minimal levels of leakiness. However, it still remains unclear how changes in the biochemical capacity of the C_4 and C_3 cycles and g_{bs} drive this acclimation.

Furthermore, nitrogen limitations may also be important for the ability of C_4 photosynthesis to effectively acclimate to low-light growth conditions. For example, nitrogen availability influenced the rates of C_4 photosynthesis and leakiness estimated with combined gas exchange and $\delta^{13}C$ measurements (Meinzer and Zhu 1998; Tazoe et al. 2006). However, direct measurements of $\Delta^{13}C$ and $\delta^{13}C$ do not always correlate, and often provide different estimates of leakiness (von Caemmerer et al. 2014; Ellsworth and Cousins 2016). This is in part because $\delta^{13}C$ is influenced by post-photosynthetic fractionations that can change over the lifetime of the leaf. Therefore, $\delta^{13}C$ is not a direct proxy for instantaneous measurements of $\Delta^{13}C$ and estimates of leakiness. As mentioned above, direct measurements of $\Delta^{13}C$ generally indicate that leakiness is low in C_4 plants; however, this has not been thoroughly tested in response to nitrogen availability and different light growth conditions.

The ability of C_4 photosynthesis to acclimate to low light and limited available nitrogen is important for assessing the use of C_4 grasses as feedstock for cellulosic biofuel programmes. For example, the C_4 grass *Miscanthus* × *giganteus* has higher yield than other bioenergy crops (Sims et al. 2006) and significant rates of carbon sequestration into the soil (Hansen et al. 2004; Clifton-Brown et al. 2007). Additionally, Miscanthus is native to Southeast Asia and its cold tolerance makes it suitable for temperate climates (Heaton et al. 2004; Naidu and Long 2004; Farage et al. 2006; Wang et al. 2008). However, in these growth environments and under dense canopies, the low light and limited nitrogen may reduce the efficiency of the C_4 concentration mechanism. Additionally, nitrogen limitations in many marginal agricultural lands may also reduce leaf growth and optimum investment in key biochemical steps within the C_4 pathway. Therefore, the aim of this study was to test how growth light intensity and nitrogen availability affect leaf anatomy, biochemistry and the efficiency of the CO_2 concentrating mechanism in *Miscanthus* × *giganteus*.

Materials and methods

Plants

Miscanthus × *giganteus* (Miscanthus) rhizomes were planted in 6-L pots and grown at Washington State University between May and the end of August 2011. We used a split-plot experimental design where the light treatment was considered the block (replicated four times) and plants within each replicate light treatment were split into the three different nitrogen treatments. The light treatment was either high-light (HL) or low-light (LL) in a temperature-controlled natural light greenhouse with daytime air temperature ranging from 25 to 28 °C and nighttime temperature from 20 to 24 °C. The LL conditions (approximately 30 % of incident radiation) were made with four replicated shade structures, each containing plants from the different nitrogen treatments. The location of all pots, including the four shade structures, was frequently changed throughout the greenhouse to avoid potential position effects of each block treatment. Additionally, the nitrogen treatments within a block were randomly arranged

and repositioned throughout the experiment. The shade structures were made of 2.1 cm diameter PVC (about 2 cubic meters) with the top and four lateral sides covered with layers of black shade cloth (Polysack Plastic Industries, Nir Yitzhak, Negev, Israel). During clear days, the midday photon flux density (PFD) on top of the pots outside the frame box was approximately 1000 and 300 μmol m^{-2} s^{-1} within for HL and LL plants, respectively. The noon daily average of solar radiation (400–1000 nm) for May, June, July and August were 667 ± 54, 680±54, 828±27, 777±17 Watts m^{-2}, respectively. Additionally, the greenhouse had large electric fans to maintain ventilation and air circulation for all plants.

Plants were watered daily and fertilized weekly with 100 ml Hoagland's solution containing 10 mM KCl, 10 mM $CaSO_4$, 75 μM Iron (Fe-EDTA), 4 mM $MgCl_2$, 0.1 mM H_3BO_4, 20 μM $MnSO_4$, 20 μM $ZnSO_4$, 4 μM $CuSO_4$, 1 μM MoO_3, 1 mM KH_2PO_4, and a controlled nitrogen amount of either 0.2, 2 or 20 mM NH_4NO_3. One and half months later, plants were given 100 ml of the same Hoagland's solution with the corresponding controlled nitrogen content every other day. The plants grown with 0.2, 2, 20 mM NH_4NO_3 are subsequently referred to as low N (LN), medium N (MN) and high N (HN) treatments, respectively. Approximately, three-month-old Miscanthus plants were used for measurements of leaf gas exchange, photosynthetic discrimination, chlorophyll content, photosynthetic enzyme activity, leaf anatomy, cell wall properties and dry matter N content. Gas exchange and discrimination measurements were made between 9 am and 4 pm local time from July 22nd to August 26th on randomly select plants within a single randomly selected block, this was repeated after all treatments within a block were measured.

CO_2 response curves and maximum phosphoenolpyruvate carboxylase activity

Gas exchange measurements were measured on the uppermost fully expanded leaves of four replicate plants per treatment in the 6 cm^2 leaf chamber of the LI-6400xt with a red–blue light-emitting diode (LI6400-02B) light source (LI-COR Inc., Lincoln, Nebraska, USA). For all measurements, a leaf temperature of 25°C and a relative humidity between 50 and 70 % were maintained. The CO_2 response curves were made at three light intensities (2000, 1000 and 300 μmol quanta m^{-2} s^{-1}) and the leaf chamber pCO_2 was varied in the following sequence: 37, 28, 19, 14, 12, 9, 8, 7, 6, 5.5, 5, 4, 19, 37, 56, 74, 93 Pa.

The initial slope of the linear part of the CO_2 response curve was used to estimate the maximum phospho*enol*pyruvate carboxylase (PEPc) activity (V_{pmax}) using the following equation (von Caemmerer 2000):

$$\text{Slope} = \frac{C_m V_{pmax}}{C_m K_p + V_{pmax}}, \quad (1)$$

where C_m is mesophyll pCO_2, which was assumed to be equal to the pCO_2 in the intercellular air space (C_i) and K_P is the Michaelis–Menten constant of PEPc for CO_2 (80 μbar).

Leaf gas exchange and online photosynthetic ^{13}C discrimination

Leaf gas exchange and online photosynthetic discrimination against $^{13}CO_2$ ($\Delta^{13}C$) were measured on the uppermost fully expanded leaves using the LI-6400xt gas exchange analyser with the opaque conifer chamber RGB light source (LI-COR 6400-18, LI-COR Inc., Lincoln, Nebraska, USA) coupled to a tunable-diode-laser absorption spectroscope (TDLAS, TGA 100A, Campbell Scientific, Logan, Utah, USA). The $^{12}CO_2$ and $^{13}CO_2$ partial pressure in the LI-COR reference and sample cells were measured by the TDLAS concurrently with a CO_2-free tank and two standard tanks (Liquid Technology Corporation, Apopka, FL, USA). The partial pressure of $^{12}CO_2$ and $^{13}CO_2$ in the reference and sample lines was calibrated using a gain and offset calculated from the two calibration tanks (Bowling et al. 2003; Ubierna et al. 2011; Sun et al. 2012, 2014). The light response curves were measured by decreasing light intensity from 2000 to 0 μmol photon m^{-2} s^{-1} with the leaf chamber at 37 Pa CO_2, leaf temperature of 25°C and relative humidity between 50 and 70 %. The simultaneous gas exchange and $\Delta^{13}C$ measurements were conducted on four individual plants of Miscanthus from each treatment, and $\Delta^{13}C$ was calculated as described by (Evans et al. 1986).

Following the gas exchange and $\Delta^{13}C$ measurements, leaves were sampled for the measurements of enzyme activities, chlorophyll content, leaf nitrogen content, leaf carbon and nitrogen isotope composition, specific leaf area (SLA) and monosaccharide composition. Leaf punches for photosynthetic enzyme activities and chlorophyll content measurements were snap-frozen in liquid nitrogen and kept at −80 °C, whereas leaf samples for total nitrogen content, carbon and nitrogen isotope composition were dried in an oven at 80 °C for 48 h. For SLA, leaves were photographed and leaf area was calculated using ImageJ (National Institutes of Health, Bethesda, MA, USA). Dry mass was measured on leaf material oven-dried at 80 °C after 48 h.

Leakiness

Leakiness (ϕ) was estimated by rearranging the equation proposed by Farquhar (1983; Farquhar and Cernusak 2012) and discussed by Ubierna et al. (2013):

$$\phi = \frac{C_{bs} - C_i}{C_i} \times \frac{\Delta^{13}C(1-t)C_a - \bar{a}(C_a - C_i) - (1+t)C_i b_4}{(1+t)[b_3 C_{bs} - s(C_{bs} - C_i)] + \bar{a}(C_a - C_i) - C_a \Delta^{13}C(1-t)}, \quad (2)$$

where C_a, C_i and C_{bs} are pCO_2 in the atmosphere, in the intercellular air spaces and in the bundle-sheath cells, respectively. Terms $\bar{a}$, b_3, b_4 and t are defined in Appendix A.

Bundle-sheath conductance (g_{bs}) was solved for each plant by finding the value that minimized the difference between the modelled and observed leaf discrimination for measurements made at 1500 and 2000 µmol quanta m^{-2} s^{-1} (Kromdijk et al. 2010; Ubierna et al. 2011). This resulted in g_{bs} values of 0.001 mol m^{-2} s^{-1} for plant from all growth conditions.

Enzyme activities and chlorophyll content

The activities of PEPc and Rubisco were measured as previously described by Cousins et al. (2006) with slight modification. For PEPc, 10 µl of leaf extract was combined with 980 µl of assay buffer (50 mM EPPS-NaOH pH 8, 10 mM $MgCl_2$, 0.5 mM EDTA, 0.2 mM NADH, 5 mM glucose-6-phosphate, 1 mM $NaHCO_3$, and 1 U ml^{-1} malate dehydrogenase) and the reaction was initiated by the addition of 10 µl of 400 mM PEP. For Rubisco, 10 µl of leaf extract was combined with 975 µl of assay buffer (50 mM EPPS-NaOH pH 8, 10 mM $MgCl_2$, 0.5 mM EDTA, 1 mM ATP, 5 mM phosphocreatine, 20 mM $NaHCO_3$, 0.2 mM NADH, 50 U ml^{-1} creatine phosphokinase, 0.2 mg carbonic anhydrase, 50 U ml^{-1} 3-phosphoglycerate kinase, 40 U ml^{-1} glyceraldehyde-3-phosphate dehydrogenase, 113 U ml^{-1} Triosephosphate isomerise, 39 U ml^{-1} glycerol 3 phosphate dehydrogenase) and the reaction was initiated by the addition of 15 µl of 34.4 mM ribulose-1,5-biphosphate (RuBP). Enzyme activity was calculated by monitoring the decrease of NADH absorbance at 340 nm with an Evolution 300 UV–VIS spectrophotometer (Thermo Fisher Scientific, Waltham, MA, USA). Additionally, the chlorophyll content was measured according to Porra et al. (1989).

Measurements of leaf anatomical traits

The measurements of leaf anatomy were carried out on mature leaves of similar age used for gas exchange measurements. Samples were fixed in 2 % (v/v) paraformaldehyde and 2 % (v/v) glutaraldehyde in 0.1 M phosphate buffer (pH 7.2), transferred subsequently to 3.5 % paraformaldehyde and 2.5 % glutaraldehyde in 0.1 M sodium cacodylate, 0.12 M sucrose, 10 mM ethylene glycol tetra-acetic acid and 2 mM magnesium chloride for overnight at 4 °C, and postfixed in 2 % (v/v) OsO_4 for 2 h at room temperature. Samples were then dehydrated in an acetone series and embedded in Spurr's epoxy resin. Cross semi-thin (1 µm) and ultra-thin (70 nm) sections were made on a Reichert Ultracut R ultramicrotome (Reichert-Jung GmbH, Heidelberg, Germany). For light microscopy, sections were stained with 1 % (w/v) Toluidine blue O in 1 % (w/v) $Na_2B_4O_7$, and studied under the Olympus BH-2 (Olympus Optical Co., Ltd.) light microscope with LM Digital Camera & Software (Jenoptik ProgRes Camera, C12plus, Jena, Germany). For transmission electron microscopy (TEM), ultra-thin cross sections were stained with 4 % (w/v) uranyl acetate followed by 2 % (w/v) lead citrate. FEI Tecnai G2 (Field Emission Instruments Company, Hillsboro, OR, USA) equipped with Eagle FP 5271/82 4K HR200KV digital camera transmission electron microscope was used for observation and photography.

Leaf and cell structural traits were characterized from cross sections (avoiding the central vein) of one mature leaf from four different individuals per treatment. Digital images were analysed with Image Analysis (UTHSCSA, version 3.0, University of Texas, San Antonio, TX, USA). The leaf thickness and interveinal distance were measured from semi-thin sections using 5–10 different fields of view for each leaf. Volume fracture of intercellular air spaces (IS) per leaf mesophyll area was calculated as a ratio of area of IS and mesophyll area (leaf section area minus epidermis and vascular tissues). The mesophyll surface area exposed to IS per unit leaf area (S_{mes}) was calculated from measurements of total length of mesophyll cell walls exposed to IS and width of section analysed with curvature correction factor as 1.34 (Evans et al. 1994). The bundle-sheath surface area per unit leaf area (S_{bs}) was measured within the interveinal distance as described by Pengelly et al. (2010) and the percentages of the bundle-sheath perimeter exposed to IS (% BS CW to IS) and percentages of bundle-sheath perimeter not covered by chloroplasts (% BS CW w/o chloroplast) were also calculated. The equations and description of these anatomical calculations are presented in the supplemental Appendix B. The mesophyll and bundle-sheath cell wall thickness was measured from TEM micrographs using at least 10 images for each leaf.

Leaf N content and $\delta^{13}C$

The oven-dried leaves were ground to a consistent powder and dried again at 80 °C for 30 min before a small sample was weighed for nitrogen content and isotope composition measurements. The percentage nitrogen was measured by combustion of samples in an elemental analyser (ECS 4010, Costech Analytical, Valencia, CA) and the isotopic composition of CO_2 and N_2 was analysed with a

continuous flow isotope ratio mass spectrometer (Delta PlusXP, Thermo Finnigan, Bremen) at Washington State University Stable Isotope Facility. Precision of repeated measurements of laboratory standard was <0.1 ‰. $\delta^{13}C$ values are reported relative to V-PDB.

Monosaccharide composition of cell wall extracts

Alcohol insoluble residue was prepared as described earlier by Harholt et al. (2006) from the same leaves used for the gas exchange measurements. Samples were hydrolyzed in 2-N-trifluoroacetic acid for 1 h at 120 °C. HPAEC-PAD analysis and quantitation of rhamnose, arabinose, galactose, glucose, xylose, galacturonic acid and glucuronic acid was performed according to ØBro et al. (2004) on an ICS 3000 (Dionex, Sunnyvale, CA) using a CarboPac PA20 (3 × 150 mm, Dionex, Sunnyvale, CA) anion exchange column.

Statistical analysis

A split-plot two-way analysis of variance (ANOVA) was conducted to evaluate differences in SLA, leaf anatomical traits, leaf N content, chlorophyll content, V_{pmax}, and leakiness among nitrogen and light treatments. Simple linear regression analysis was conducted to evaluate relationships between rate of CO_2 assimilation and leaf N content, leakiness and leaf N content, chlorophyll content and leaf N content, as well as rate of CO_2 assimilation and chlorophyll content. All statistical analyses were carried out using Statistix version 9.0 (Analytical Software, Tallahassee, FL, USA).

Results

Leaf anatomical traits

Leaf thickness was greater in high-light (HL) compared to low-light (LL) plants and generally increased with leaf nitrogen (Fig. 1a, b; Table 1). Additionally, the specific leaf area (SLA; leaf area per unit dry mass) was lower under HL compared to LL plants but was not significantly affected by nitrogen (Table 1). The interveinal distance was greater under HL compared to LL but was not affected by nitrogen (Fig. 1a, b; Table 1). The mesophyll surface area exposed to the intercellular airspace per unit leaf area (S_{mes}; m^2 m^{-2}) was greater in HL compared to LL but was not affected by nitrogen (Table 1). Additionally, the bundle-sheath area per unit leaf area (S_{bs}; m^2 m^{-2}) was larger in HL compared to LL plants and increased with nitrogen (Table 1). The percentage of the bundle-sheath perimeter exposed to IS (% BS CW to IS) was not affected by the growth conditions, while the percentages of bundle-sheath perimeter not covered by chloroplasts (% BS CW w/o chloroplast) were lower in HL as a result of sparse chloroplast distribution in bundle-sheath under LL conditions (Table 1). Additionally, the bundle-sheath cell wall thickness was significantly greater in the HL compared to LL grown plants but did not change with nitrogen (Table 1); however, the mesophyll cell wall thickness was not affected by either condition. The leaf cell wall sugar composition varied slightly with rhamnose and xylose content changing with nitrogen, while only galacturonic acid was significantly different between HL and LL plants (Table 1).

Leaf chlorophyll, nitrogen, carbon isotope composition and enzyme activity

The HL plants had less chlorophyll (mmol m^{-2}) relative to the LL plants and the content increased with nitrogen in both HL and LL (Table 2); however, the chlorophyll a/b was insensitive to light treatments but decreased with nitrogen (Table 2). The total N per unit leaf area was significantly affected by both nitrogen and light treatments, with the leaf N content in HL-HN leaves higher than leaves from all other treatments (Table 2). Under HL, the carbon isotope composition ($\delta^{13}C$) of dried leaves was more enriched than the LL treatment; however, $\delta^{13}C$ was more depleted with increasing nitrogen availability in both HL and LL plants (Table 2). The in vitro activity of both PEPc and Rubisco was greater in HL compared to LL plants, and increased with nitrogen availability; however, PEPc/Rubisco ratio increased only with light and not nitrogen (Table 2).

Net CO_2 assimilation in response to changing CO_2 concentrations

The CO_2-saturated rate of net CO_2 assimilation (A_{sat}) in the HL-HN compared to LL–HN plants was significantly higher under 2000 µmol quanta m^{-2} s^{-1} (30.2 ± 0.7 vs. 21.0 ± 2.2 µmol m^{-2} s^{-1}) and 1000 µmol quanta m^{-2} s^{-1} (23.9 ± 1.1 vs. 16.36 ± 1.8 µmol m^{-2} s^{-1}) but had only slightly higher rates at 300 µmol quanta m^{-2} s^{-1} (12.2 ± 0.5 vs. 10.2 ± 0.8 µmol m^{-2} s^{-1}) (Fig. 2 a, d). In the MN and LN grown plants, A_{sat} was similar between HL and LL grown plants regardless of the measurement light intensities (Fig. 2b vs. e, c vs. f). Values of A_{sat} decreased with reduced nitrogen availability regardless of growth light conditions; however, the response was greater in the HL compared to LL plants (Fig. 2). The maximum PEPc carboxylase activity (V_{pmax}) determined from the initial slope of the CO_2 response curves measured under

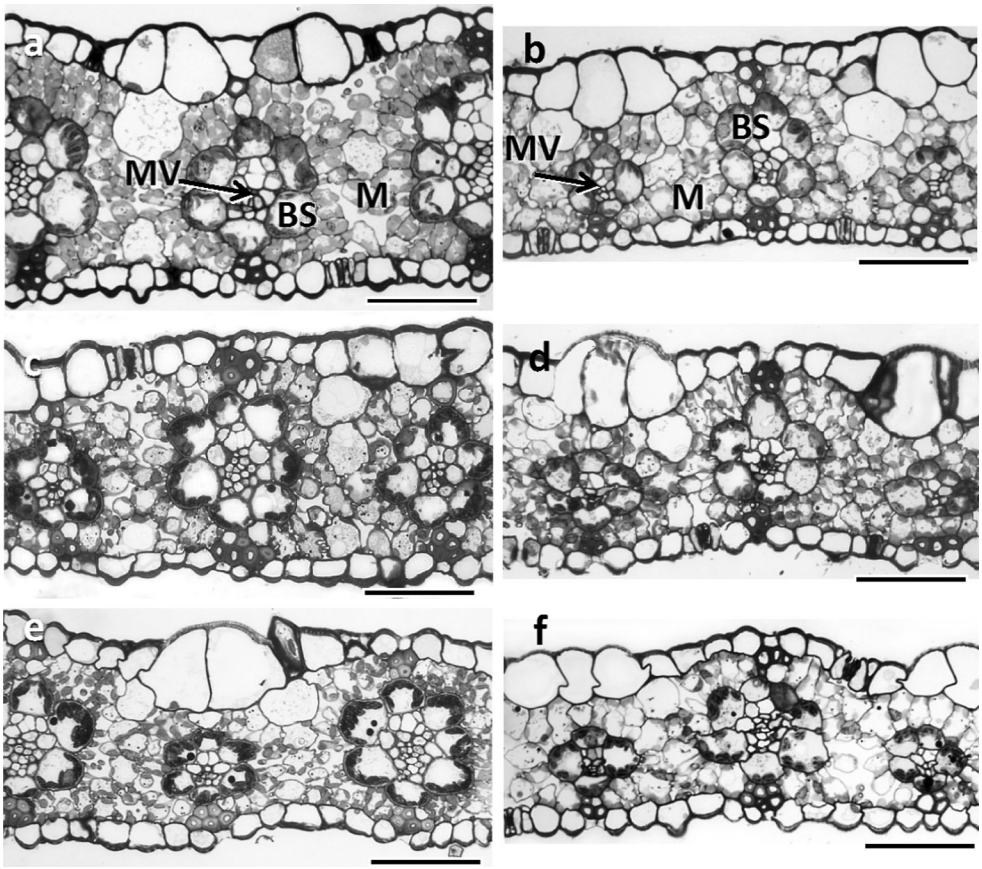

Fig. 1 Leaf cross sections (**a**–**f**) in *Miscanthus* × *giganteus* grown at two different irradiances of 1000 µmol quanta m^{-2} s^{-1} (high light, **a**, **c**, **e**) and 300 µmol quanta m^{-2} s^{-1} (low light, **b**, **d**, **f**), and different nitrogen conditions, high N (**a**, **b**), medium N (**c**, **d**) and low N (**e**, **f**). Scales: 50 µm

2000 µmol quanta m^{-2} s^{-1} and using Eq. (1) increased with nitrogen in both HL and LL (Table 2), and was significantly higher under HL compared to LL regardless of nitrogen treatment (Table 2).

Photosynthetic carbon isotope discrimination in response to light

In all plants, the net rate of CO_2 assimilation (A_{net}) increased with light intensity (Fig. 3a, b). In the HL plants, A_{net} measured above 500 µmol quanta m^{-2} s^{-1} was higher in the HN treatment compared to MN and LN treatments; however, below this measurement light intensity, there was no difference in A_{net} between nitrogen treatments for the HL plants. In the LL grown plants, there was not a significant difference in A_{net} between nitrogen treatments across all the measurement light intensities. Overall, A_{net} was higher in HL compared to LL grown plants regardless of nitrogen treatment (Fig. 3a, b).

The photosynthetic carbon isotope discrimination ($\Delta^{13}C$) decreased with irradiance for both HL and LL grown plants, regardless of nitrogen treatments (Fig. 3c, d). However, leakiness (ϕ) calculated using Eq. (4) was relatively constant in response to changes in the measurement light intensities in all plants. However, in the LL–MN and LL–LN plants, values of ϕ increased under the lowest measuring condition of 60 µmol quanta m^{-2} s^{-1}. In general, leakiness across all measured light conditions was slightly lower in HL-HN plants compared to plants from all other treatments (Fig. 3e, f).

Correlations between leaf nitrogen content, A_{net} and leakiness

There was a positive correlation of A_{net} (Fig. 4a; $r^2 = 0.93$, $P = 0.001$) and (Fig. 4b; $r^2 = 0.72$, $P = 0.033$) with total leaf N. This was primarily driven by the fact that A_{net} (31.2 ± 0.7 µmol m^{-2} s^{-1}) was significantly higher and ϕ (0.26 ± 0.01) significantly lower in the HL-HN plants compared to plants from the other treatments. The values of A_{net} and ϕ taken from measurements at 2000 µmol quanta m^{-2} s^{-1} are presented in Fig. 3.

Table 1 Leaf anatomical properties of *Miscanthus* × *giganteus* grown at two different irradiances of 1000 (High light) and 300 μmol quanta m^{-2} s^{-1} (Low light), and three different nitrogen conditions (High N, HN; Medium N, MN; Low N, LN)

Nitrogen	High light			Low light			Significance		
	HN	MN	LN	HN	MN	LN	L	N	N × L
Leaf thickness (μm)	115.9 ± 2.2	105.6 ± 1.7	95.2 ± 3.7	89.6 ± 3.9	86.9 ± 1.0	84.8 ± 3.3	**	**	ns
SLA (m^2kg^{-1})	22.6 ± 1.0	25.0 ± 0.8	25.9 ± 1.6	33.1 ± 0.4	32.2 ± 0.3	31.2 ± 0.3	**	ns	ns
Interveinal distance (μm)	98.2 ± 2.8	90.8 ± 2.9	95.3 ± 2.6	83.1 ± 3.3	84.5 ± 2.7	74.0 ± 3.2	**	ns	ns
S_{mes} (m^2 m^{-2})	9.7 ± 0.6	8.5 ± 0.2	9.7 ± 0.2	6.9 ± 0.3	6.1 ± 0.2	5.3 ± 0.3	**	ns	ns
S_{bs} (m^2 m^{-2})	2.0 ± 0.05	1.9 ± 0.01	1.7 ± 0.03	1.8 ± 0.08	1.7 ± 0.03	1.7 ± 0.01	*	*	ns
% BS CW to IS	16.6 ± 1.7	13.9 ± 0.3	25.5 ± 2.4	14.9 ± 3.9	15.8 ± 2.4	13.9 ± 4.0	ns	ns	ns
% BS CW w/o chloroplast	8.6 + 1.4	6.8 + 0.4	4.0 + 0.6	20.3 + 3.1	18.7 + 4.3	27.5 + 5.4	*	ns	ns
Cell wall thickness (μm)									
Mesophyll	0.17 ± 0.001	0.23 ± 0.03	0.22 ± 0.01	0.20 ± 0.02	0.20 ± 0.002	0.19 ± 0.02	ns	ns	ns
Bundle-sheath	0.91 ± 0.01	1.00 ± 0.03	1.16 ± 0.02	0.74 ± 0.06	0.87 ± 0.04	0.73 ± 0.08	**	ns	ns
Rhamnose (mol%)	0.65 ± 0.11[a]	0.45 ± 0.02[b]	0.42 ± 0.06[b]	0.51 ± 0.12[b]	0.50 ± 0.02[b]	0.48 ± 0.04[b]	ns	**	*
Arabinose (mol%)	16.5 ± 0.7	17.4 ± 0.1	16.8 ± 0.5	16.8 ± 0.5	17.6 ± 0.4	17.2 ± 0.1	ns	ns	ns
Galactose (mol%)	4.2 ± 0.2[a]	3.1 ± 0.1[b]	3.2 ± 0.2[b]	4.0 ± 0.4[a]	4.3 ± 0.1[a]	4.0 ± 0.3[a]	*	*	**
Glucose (mol%)	12.8 ± 0.9	10.4 ± 0.7	13.5 ± 1.5	11.6 ± 0.6	9.6 ± 1.0	12.3 ± 1.3	ns	ns	ns
Xylose (mol%)	61.2 ± 0.5	65.1 ± 0.5	62.2 ± 1.5	62.1 ± 0.5	63.3 ± 0.7	61.1 ± 0.6	ns	**	ns
Galacturonic acid (mol%)	4.3 ± 1.0	3.2 ± 0.2	3.6 ± 0.5	4.5 ± 0.5	4.1 ± 0.3	4.4 ± 0.5	*	ns	ns
Glucuronic acid (mol%)	0.47 ± 0.01	0.33 ± 0.08	0.37 ± 0.07	0.42 ± 0.05	0.48 ± 0.05	0.45 ± 0.10	ns	ns	ns

Data are reported as the arithmetic mean ± 1 standard error ($n = 4$). Significance tested with a split-plot ANOVA where nitrogen (N) was nested within the growth light treatments (L). LSD post hoc test was conducted only when interaction of N × L was significant ($P < 0.05$). Similar superscripted letters indicate non-significant differences between treatments ($P > 0.05$)

SLA specific leaf area, leaf area/leaf dry mass, *ns* = not significant

* $P < 0.05$, ** $P < 0.01$

Table 2 Leaf parameters of *Miscanthus* × *giganteus* grown at two different irradiances of 1000 (High light) and 300 µmol quanta m^{-2} s^{-1} (Low light) and three nitrogen conditions (High N, HN; Medium N, MN; Low N, LN)

High light				Low light			Significance		
Nitrogen	HN	MN	LN	HN	MN	LN	L	N	L × N
Chlorophyll a + b (mmol m^{-2})	0.43 ± 0.06	0.23 ± 0.03	0.17 ± 0.01	0.45 ± 0.05	0.39 ± 0.04	0.26 ± 0.05	**	**	ns
Chlorophyll a/b	3.09 ± 0.11	3.38 ± 0.08	3.84 ± 0.45	2.94 ± 0.12	3.09 ± 0.07	3.6 ± 0.3	ns	*	ns
Leaf nitrogen (mmol m^{-2})	98.9 ± 7.3^{a}	44.9 ± 2.9^{bcd}	39.7 ± 2.9^{d}	58.3 ± 1.1^{b}	53.3 ± 3.4^{bc}	43.4 ± 2.6 ^{cd}	*	**	**
Dry matter $\delta^{13}C$ (‰)	−12.5 ± 0.02	−12.2 ± 0.18	−12.0 ± 0.09	−13.0 ± 0.06	−12.5 ± 0.15	−12.3 ± 0.03	**	**	ns
PEPc activity (µmol HCO_3^- m^{-2} s^{-1})	101.8 ± 7.2^{a}	58.0 ± 6.3^{b}	45.3 ± 2.6^{bc}	58.9 ± 1.4^{b}	45.4 ± 3.6^{bc}	35.9 ± 4.0^{c}	**	**	**
Rubisco activity (µmol CO_2 m^{-2} s^{-1})	34.9 ± 2.4^{a}	19.8 ± 2.5^{bc}	15.1 ± 0.8^{bd}	22.1 ± 0.5^{c}	19.4 ± 0.8^{bcd}	15.2 ± 1.1^{d}	**	**	**
PEPc/Rubisco	2.9 ± 0.3	2.96 ± 0.15	3.02 ± 0.23	2.67 ± 0.06	2.34 ± 0.11	2.4 ± 0.2	**	ns	ns
V_{pmax} (µmol m^{-2} s^{-1})	39.9 ± 1.7	27.95 ± 1.17	24.17 ± 0.81	27.6 ± 3.6	25.8 ± 0.7	21.30 ± 1.31	*	**	ns

Data are the mean ± 1 standard error ($n = 4$). Significance tested with a split-plot ANOVA where nitrogen (N) was nested within the growth light treatments (L). LSD post hoc test was conducted only when interaction of N × L was significant ($P < 0.05$). Similar superscripted letters indicate non-significant differences between treatments ($P > 0.05$)

PEPc phospho*enol*pyruvate carboxylase, *Rubisco* ribulose-1,5-bisphosphate carboxylase/oxygenase, *C* leaf organic content, *ns* not significant, V_{pmax} the maximum rate of phospho*enol*pyruvate carboxylase determined from gas exchange

* $P < 0.05$, ** $P < 0.01$

Discussion

There is limited information on how light and nitrogen availability influence leaf anatomy, biochemistry and the efficiency of the CO_2 concentrating mechanism in C_4 grasses. Below we discuss how measurements of microscopy, biochemistry and leaf CO_2 isotope exchange where used to determine how changes in leaf anatomy and biochemistry influence the efficiency of C_4 photosynthesis in Miscanthus grown under different light and nitrogen treatments.

Leaf structure and CO_2 movement

In C_3 plants, mesophyll conductance to CO_2 (g_m) restricts substrate availability to Rubisco within the mesophyll chloroplast (Flexas et al. 2014). However, in C_4 plants, it is typically assumed that g_m has to be large to maintain the high rates of CO_2 assimilation, particularly when intercellular CO_2 concentrations are low as in many C_4 grasses (von Caemmerer et al. 2008, 2014). The mesophyll surface area exposed to the intercellular airspace per unit leaf area (S_{mes}) and cell wall thickness have been implicated in determining g_m in both C_3 and C_4 plants (Evans et al. 1994; Pengelly et al. 2010; von Caemmerer et al. 2014). In fact, changes in these parameters due to growth conditions significantly influence g_m in C_3 plants; however, there is little information on the response of g_m in C_4 plants (Gillon and Yakir 2000). The increase in S_{mes} without changes in mesophyll cell wall thickness in the HL compared to the LL grown plants suggests that g_m is higher in plants with greater photosynthetic capacity. This would minimize the drawdown of CO_2 between the intercellular air space and the mesophyll cytoplasm to enhance HCO_3^- availability to PEPc to maintain rates of CO_2 assimilation. Unfortunately, unlike in C_3 plants, the use of $\Delta^{13}CO_2$ is not able to resolve g_m in C_4 plants.

Similarly, bundle-sheath CO_2 conductance (g_{bs}) is in part influenced by the bundle-sheath surface area per unit leaf area (S_{bs}) and the bundle-sheath cell wall thickness (von Caemmerer and Furbank 2003). Values of g_{bs} are not directly measurable and are therefore typically estimated, with certain assumptions, from combined measurements of gas exchange, stable isotope analysis and chlorophyll fluorescence (Bellasio and Griffiths 2014a; Kromdijk et al. 2014; Yin et al. 2016). The value of g_{bs} can have a strong influence on the efficiency of the CO_2 concentrating mechanism; therefore, changes in S_{bs} or the bundle-sheath cell wall thickness in response to changes in growth conditions may directly impact leakiness. In the HL plants, the bundle-sheath cell wall thickness and S_{bs} were greater than in LL plant suggesting that any increase in g_{bs} potentially

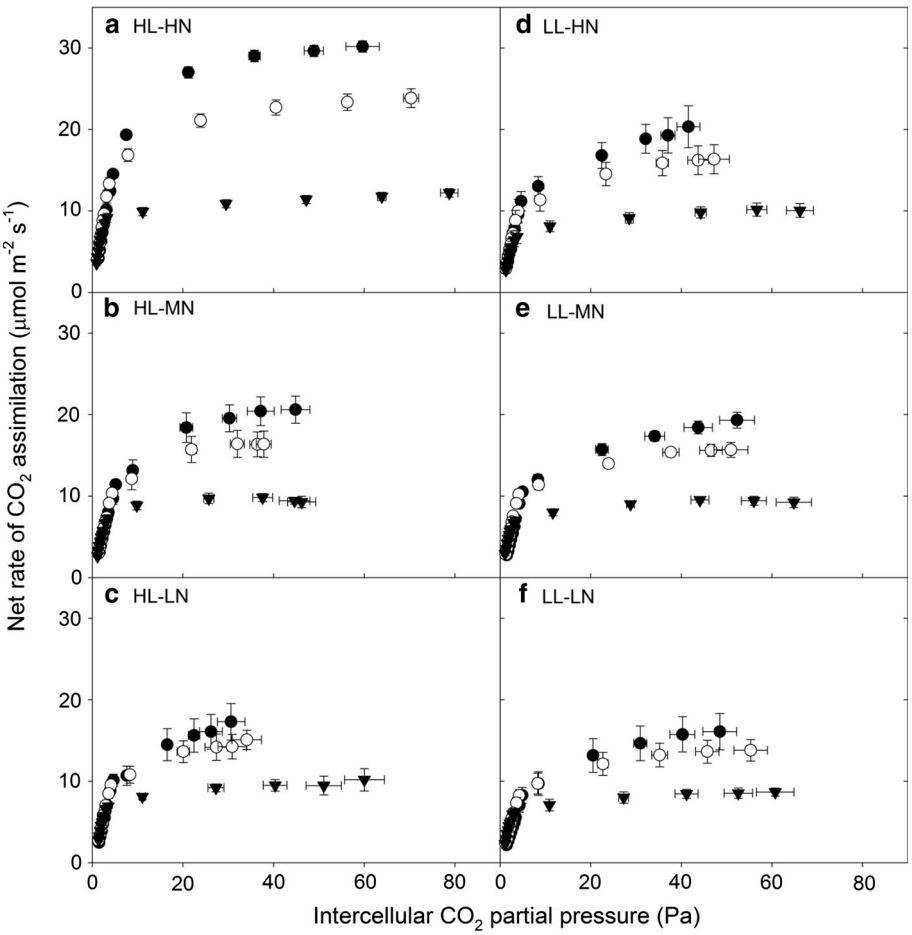

Fig. 2 Net rate of CO_2 assimilation in response to CO_2 partial pressure (C_i) under different measurement light intensities of 2000 (*filled circles*), 1000 (*open circles*) and 300 (*inverse triangles*) μmol quanta m^{-2} s^{-1} in plants grown at 1000 (HL) and 300 μmol quanta m^{-2} s^{-1} (LL), and three different nitrogen conditions (High N, HN; Medium N, MN; Low N, LN). Leaf temperature and leaf chamber relative humidity were controlled at 25 °C and 50–70 %, respectively. Data are reported as the arithmetic mean ± 1 standard error ($n = 4$)

caused by changes in S_{bs} is offset by the increase in cell wall thickness. Additionally, the bundle-sheath cell area (data not shown) was larger in the HL compared to LL plants, which likely influenced the increased interveinal distance in HL plants. However, compared to the HL plants, the percentages of bundle-sheath perimeter not covered by chloroplasts (% BS CW w/o chloroplast) in the LL plants were greater, which may increase the lose of CO_2 from the bundle-sheath cells. The nitrogen treatment did not significantly increased cell wall thickness but S_{bs} did significantly increase with nitrogen, which suggests that g_{bs} would be higher in plants with increasing leaf nitrogen. Although there were significant differences in the content of some cell wall monosaccharides (Table 2), the actual percentage change between growth treatments was small. However, the changes in rhamnose, galacturonic acid and galactose are likely to affect the composition of pectin (Scheller et al. 2007), which could influence the diffusion properties of the mesophyll or bundle-sheath cell walls. As discussed below, is influenced by both g_{bs} and the biochemical capacity of the C_3 and C_4 cycle. Therefore, the potential change in g_{bs} due to changes in the bundle-sheath cells may be compensated by changes in leaf metabolism in order to maintain ϕ under these growth conditions.

C_4 Biochemistry

In general, the extractable rates of in vitro PEPc and Rubisco activity were greater in HL versus LL plants and increased with leaf nitrogen increased (Table 2). However, as with rates of net CO_2 assimilation (Figs. 2, 3), the difference in PEPc and Rubisco activities was not significantly different between HL and LL plants with low leaf nitrogen (MN and LN). This suggests that limited nitrogen availability can diminish the potential biochemical acclimation of C_4 photosynthesis to high-light conditions. Additionally, under low-light conditions, C_4 photosynthesis is not able to take advantage of the increased nitrogen availability. Interestingly, the PEPc/Rubisco ratio was not influenced by the nitrogen treatments, regardless of growth light conditions and PEPc/Rubisco was higher in the HL compared to LL plants. This indicates that regardless of leaf nitrogen, the partitioning of nitrogen between PEPc and Rubisco remained constant suggesting a constant potential capacity for these steps of the C_4 and the C_3 cycle, respectively. However, in the HL plants, the balance of PEPc/Rubisco increased compared to LL plants suggesting a greater capacity of the C_4 cycle compared to the Rubisco-driven C_3 pathway. If the in vitro activities of

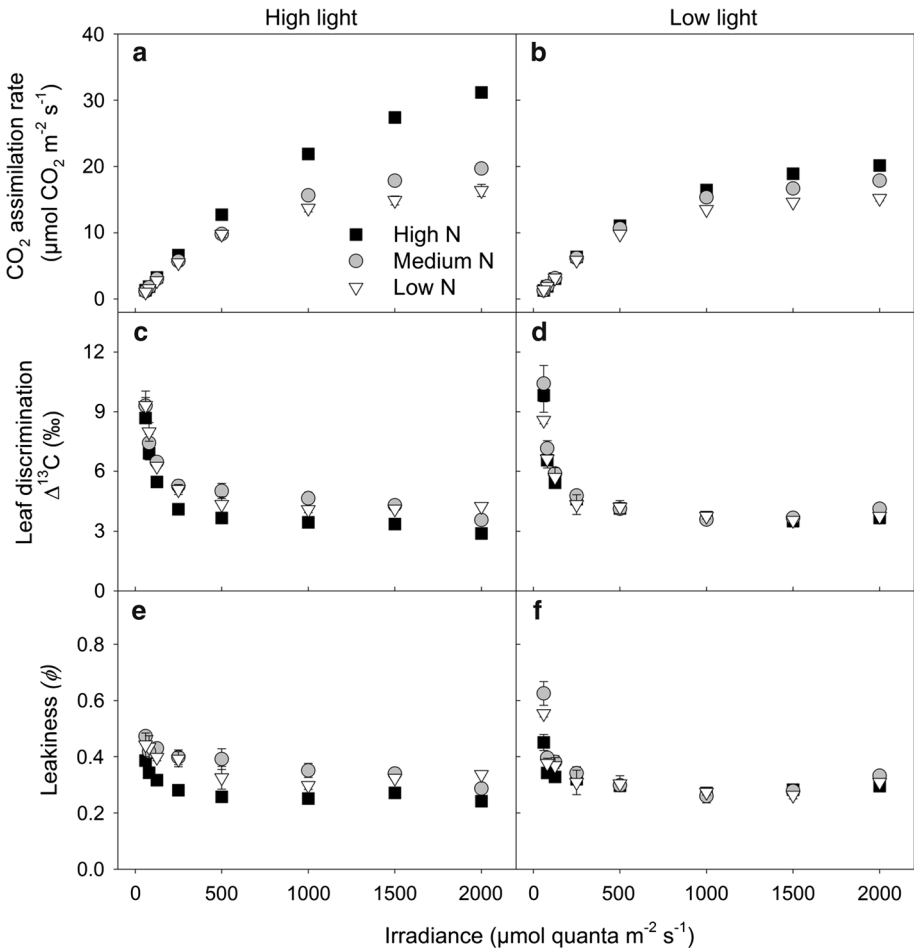

Fig. 3 Net CO_2 assimilation rate, (**a**) and (**b**), carbon isotope discrimination ($\Delta^{13}C$), (**c**) and (**d**), and bundle-sheath leakiness (ϕ), (**e**) and (**f**), as a function of irradiance, in *Miscanthus* × *giganteus* grown at two different irradiances of 1000 (high light) and 300 μmol quanta m^{-2} s^{-1} (low light), and three different nitrogen conditions (high N, *square*; medium N, *circle*; low N, *triangle*). Measurements were made at an ambient pCO_2 of ~35 Pa, and a leaf temperature of 25 °C. Data are reported as the arithmetic mean ± 1 standard error ($n = 4$)

these enzymes are proxies for the capacity of the C_4 and C_3 cycles, respectively, then all else being equal this would suggest a potential over cycling of the CO_2 concentrating mechanism and an increase in leakiness. However, the HL plants in the HN treatment had decreased values of leakiness, which as mentioned above is determined by both the capacity of the C_4 and C_3 cycles as well as g_{bs}. It is therefore likely that the change in PEPc/Rubisco in the HL and HN plants was offset by a decrease in g_{bs}, which would minimize leakiness. However, it should be noted that the extractable maximum activities of PEPc and Rubisco might not accurately depict the in vivo regulated rates.

For example, the in vivo estimates of V_{pmax} determined from the initial slope of the CO_2 response curves (see Eq. 1) are significantly less than the in vitro PEPc activity, regardless of growth condition. This suggests either significant regulation of leaf PEPc activity and the enzyme is not 100 % active or the in vivo estimates are under represented. Based on a sensitivity analysis of parameters in Eq. (1), only errors in the measurements of net CO_2 assimilation (A_{net}) or the mesophyll CO_2 partial pressure (C_m) would be sufficient to alter in vivo V_{pmax} to match the in vitro values. While the measurements of A_{net} could be off, it is unlikely they are systematically erroneous. It is more likely that the values of C_m which are derived from $C_m = C_i - A/g_m$ are incorrectly estimated due to uncertainties of g_m. It is typically assumed that g_m is high in C_4 plants and tends not to restrict CO_2 availability to the mesophyll cells. However, it is difficult to estimate g_m in C_4 plants and theoretically g_m could be relatively low as in C_3 plants, which would lower the estimated values of C_m. If g_m were low then the assumptions used here that $C_m = C_i$ would be invalid and the derived V_{pmax} from Eq. (1) would be significantly higher. As mentioned before, g_m in C_4 plants is difficult to measure with $\Delta^{13}C$; however, future analysis of g_m in C_4 plants could be investigated with combined measurements of $\Delta^{18}O$ and the isotopic signature of transpired water (Gillon and Yakir 2000; von Caemmerer et al. 2014; Barbour et al. 2016).

Leaf carbon isotopic signature and CO_2 exchange

The leaf carbon isotopic signature ($\delta^{13}C$) was more depleted in LL compared to HL plants and $\delta^{13}C$ became

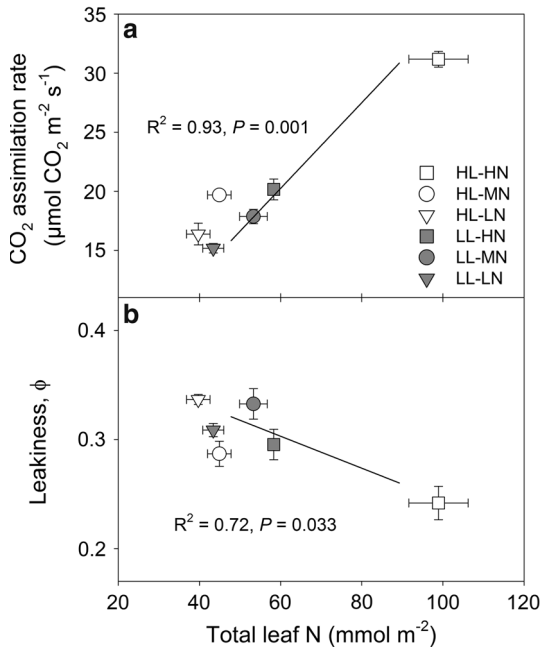

Fig. 4 Relationship between total leaf N (mmol m^{-2}) and **a** Net CO_2 assimilation rate (A_{net}; µmol CO_2 m^{-2} s^{-1}), and **b** bundle-sheath leakiness (ϕ), in *Miscanthus* × *giganteus* grown at two different irradiances of 1000 (High light, *open symbols*) and 300 µmol quanta m^{-2} s^{-1} (Low light, *filled symbols*), and three different nitrogen conditions (High N, *square*; Medium N, *circle*; Low N, *triangle*). The measurements of A_{net} and ϕ are taken from Fig. 3 at 2000 µmol quanta m^{-2} s^{-1}. Data are reported as the arithmetic mean ± 1 standard error ($n = 4$)

more depleted as leaf nitrogen increased (Table 1). In C_4 plants, one of the potential driving factors influencing $\delta^{13}C$ is the efficiency of the CO_2 concentrating mechanism and leakiness. Therefore, the $\delta^{13}C$ differences suggest leakiness is greater in LL compared to HL plants and increases with leaf nitrogen. However, recent comparisons of $\delta^{13}C$ and estimates of leakiness from measurements of leaf CO_2 isotope exchange ($\Delta^{13}C$) suggest that variation in $\delta^{13}C$ does not always correspond to changes in $\Delta^{13}C$ (Cousins et al. 2008; Kromdijk et al. 2014; von Caemmerer et al. 2014). In fact as discussed below, the $\Delta^{13}C$ and the corresponding leakiness were slightly lower in the HL-HN grown plants compared to plants from the other growth conditions; however, there was not a significant difference in leakiness between HL and LL plants across all nitrogen treatments.

Alternatively, $\delta^{13}C$ differences could be caused by post-photosynthetic fractionation. However, conservation of mass requires that there must be a loss of carbon from the leaf, for example, via respiration or export from the leaf to influence $\delta^{13}C$. Therefore, differences in the CO_2 released during respiration between plants from the different growth conditions could influence leaf $\delta^{13}C$ (Ghashghaie et al. 2001). However, the rates of dark respiration were not significantly different between plants from the various growth conditions (data not shown) and the rates were an order of magnitude lower than rates of CO_2 assimilation. Therefore, the isotopic fractionation of respiration would have to be unrealistically different between plants. For modelling, $\delta^{13}C$ values of respiratory fractionation were not directly measured but estimated as described in Appendix A; however, a sensitivity analysis indicated that even extreme values would not drive the $\Delta^{13}C$ shift seen between treatments. Unfortunately, there are limited data in the literature on how respiratory fractionation varies between C_4 plants, particularly in response to changing environmental conditions. Therefore, further research is needed to determine the influence of leaf respiration on $\Delta^{13}C$.

Photosynthetic efficiency

The efficiency of the CO_2 concentrating mechanism in C_4 plants cannot be directly measured; however, through modelling and measurements of $\Delta^{13}C$ the efficiency can be estimated from calculations of leakiness (see Eq. 2; Ubierna et al. 2011; Kromdijk et al. 2014; von Caemmerer et al. 2014). There has been a significant discussion in the literature about the sensitivity of leakiness to changes in environmental conditions, particularly under low-light growth and measurement conditions. Early measurements suggested that leakiness increased under low-light measuring conditions estimated from both of $\Delta^{13}C$ and combined gas exchange with fluorescence measurements (Henderson et al. 1992; Cousins et al. 2006; Tazoe et al. 2006; Kubásek et al. 2007; Cousins et al. 2008; Kromdijk et al. 2008; Tazoe et al. 2008; Kromdijk et al. 2010). However, more recent estimates using $\Delta^{13}C$ and taking into account the full model of C_4 leaf CO_2 isotope exchange suggest leakiness changes only slightly under the lowest light measurements conditions (Ubierna et al. 2011, 2013; Kromdijk et al. 2014). Additionally, C_4 plants grown under low light acclimate to these conditions and have lower leakiness under low light compared to higher light grown plants (Pengelly et al. 2010; Bellasio and Griffiths 2014a, b, c; Kromdijk et al. 2014). It is important to note that leakiness at very low light is difficult to estimate because measurements are confounded by the influence of respiration in the light, especially from the bundle-sheath mitochondria. Therefore, the leakage of CO_2 from the bundle-sheath cells under low light may relate to both the CO_2 concentrating mechanism and day respiration, the later not directly related to leakiness (Kromdijk et al. 2014; Sage 2014). Here the estimates of leakiness were similar across all growth conditions, except for in the HL and HN plants, which had slightly lower leakiness under all measurement light intensities (Fig. 4). The response of leakiness to decreasing measurement light intensities was

relatively small except for in the LN plants at the lowest measurement light intensity. These estimates suggest that the CO_2 concentrating mechanism in Miscanthus is robust under these growth conditions, and that the observed changes in leaf anatomy and biochemistry likely help to maintain this efficiency.

Conclusions

The growth of Miscanthus under different light and nitrogen treatments has a strong influence on the leaf anatomy and the levels of extractable PEPc and Rubisco activities. Additionally, the net rates of CO_2 assimilation were typically lower under the LL treatment expect in the plants with the lowest leaf nitrogen. Taken together these data suggest that photosynthesis and leaf anatomy in Miscanthus are influenced by an interaction of both light availability and leaf nitrogen. However, the measurements of $\Delta^{13}C$ and modelled estimates of leakiness suggest that the efficiency of the CO_2 concentrating mechanism in Miscanthus is robust, even when environmental growth conditions drive changes in leaf anatomy and biochemistry.

Acknowledgments This research was supported by the National Natural Science Foundation of China [Grant Nos. 41071032, 31270445], the 9th Thousand Talents Program of China, the US Department of Energy, Office of Basic Energy Science [DE-FG02_09ER16062] and Office of Science, Office of Biological and Environmental Research [DE-AC02-05CH11231]. Instrumentation was obtained through an NSF Major Research Instrumentation Grant [#0923562]. JLH was supported by an Australian Research Council Future Fellowship [FT130101165]. We thank C. Cody for plants growth management, Dr. Steve Long for Miscanthus plant material and the Franceschi Microscopy and Imaging Center of Washington State University for use of its facilities.

References

Barbour MM, Evans JR, Simonin KA, von Caemmerer S (2016) Online CO_2 and H_2O oxygen isotope fractionations allows estimation of mesophyll conductance in C_4 plants, and reveals that mesophyll conductance decreases as leaves age in both C_4 and C_3 plants. New Phytologist

Bellasio C, Griffiths H (2014a) Acclimation of C_4 metabolism to low light in mature maize leaves could limit energetic losses during progressive shading in a crop canopy. J Exp Bot 65:3725–3736

Bellasio C, Griffiths H (2014b) Acclimation to low light by C_4 maize: implications for bundle sheath leakiness. Plant Cell Environ 37:1046–1058

Bellasio C, Griffiths H (2014c) The operation of two decarboxylases, transamination, and partitioning of C_4 metabolic processes between mesophyll and bundle sheath cells allows light capture to be balanced for the maize C4 pathway. Plant Physiol 164:466–480

Bowling DR, Sargent SD, Tanner BD, Ehleringer JR (2003) Tunable diode laser absorption spectroscopy for stable isotope studies of ecosystem-atmosphere CO_2 exchange. Agric For Meteorol 118:1–19

Clifton-Brown JC, Breuer J, Jones MB (2007) Carbon mitigation by the energy crop, *Miscanthus*. Glob Change Biol 13:2296–2307

Cousins AB, Badger MR, Von Caemmerer S (2006) Carbonic anhydrase and its influence on carbon isotope discrimination during C_4 photosynthesis. Insights from antisense RNA in Flaveria bidentis. Plant Physiol 141:232–242

Cousins AB, Badger MR, von Caemmerer S (2008) C_4 photosynthetic isotope exchange in NAD-ME- and NADP-ME-type grasses. J Exp Bot 59:1695–1703

Ellsworth PZ, Cousins AB (2016) Carbon isotopes and water use efficiency in C_4 plants. Curr Opin Plant Biol 31:155–161

Evans JR, Sharkey TD, Berry JA, Farquhar GD (1986) Carbon isotope discrimination measured concurrently with gas exchange to investigate CO_2 diffusion in leaves of higher plants. Aust J Plant Physiol 13:281–292

Evans JR, von Caemmerer S, Setchell BA, Hudson GS (1994) The Relationship between CO_2 Transfer Conductance and Leaf Anatomy in Transgenic Tobacco with a Reduced Content of Rubisco. Aust J Plant Physiol 21:475–495

Farage PK, Blowers D, Long SP, Baker NR (2006) Low growth temperatures modify the efficiency of light use by photosystem II for CO_2 assimilation in leaves of two chilling-tolerant C_4 species, *Cyperus longus* L. and *Miscanthus* x *giganteus*. Plant Cell Environ 29:720–728

Farquhar GD (1983) On the nature of carbon isotope discrimination in C_4 species. Aust J Plant Physiol 10:205–226

Farquhar GD, Cernusak LA (2012) Ternary effects on the gas exchange of isotopologues of carbon dioxide. Plant Cell Environ 35:1221–1231

Flexas J, Carriqui M, Coopman RE, Gago J, Galmes J, Martorell S, Morales F, Diaz-Espejo A (2014) Stomatal and mesophyll conductances to CO_2 in different plant groups: underrated factors for predicting leaf photosynthesis responses to climate change? Plant Sci 226:41–48

Ghashghaie J, Duranceau M, Badeck F-W (2001) $\delta^{13}C$ of CO_2 respired in the dark in relation to $\delta^{13}C$ of leaf metabolites: comparison between *Nicotiana sylvestris* and *Helianthus annuus* under drought. Plant Cell Environ 24:505–515

Gillon JS, Yakir D (2000) Naturally low carbonic anhydrase activity in C_4 and C_3 plants limits discrimination against $(COO)\text{-}O^{18}$ during photosynthesis. Plant Cell Environ 23:903–915

Hansen EM, Christensen BT, Jensen LS, Kristensen K (2004) Carbon sequestration in soil beneath long-term *Miscanthus* plantations as determined by C^{13} abundance. Biomass Bioenergy 26:97–105

Harholt J, Jensen JK, Sorensen SO, Orfila C, Pauly M, Scheller HV (2006) ARABINAN DEFICIENT 1 is a putative arabinosyltransferase involved in biosynthesis of pectic arabinan in Arabidopsis. Plant Physiol 140:49–58

Hatch MD, Slack CR, Johnson HS (1967) Further studies on a new pathway of photosynthetic carbon dioxide fixation in sugarcane and its occurence in other plant species. Biochem J 102:417–422

Hatch MD, Agostino A, Jenkins CLD (1995) Measurement of the leakage of CO_2 from bundle-sheath cells of leaves during C_4 photosynthesis. Plant Physiol 108:173–181

Heaton EA, Long SP, Voigt TB, Jones MB, Clifton-Brown J (2004) *Miscanthus* for renewable energy generation: European Union experience and projections for Illinois. Mitig Adapt Strat Glob Change 9:433–451

Henderson SA, von Caemmerer S, Farquhar GD (1992) Short-Term Measurements of Carbon Isotope Discrimination in Several C_4 Species. Aust J Plant Physiol 19:263–285

Kromdijk J, Schepers HE, Albanito F, Fitton N, Carroll F, Jones MB, Finnan J, Lanigan GJ, Griffiths H (2008) Bundle Sheath

Leakiness and Light Limitation during C_4 Leaf and Canopy CO2 Uptake. Plant Physiol 148:2144–2155

Kromdijk J, Griffiths H, Schepers HE (2010) Can the progressive increase of C_4 bundle sheath leakiness at low PFD be explained by incomplete suppression of photorespiration? Plant Cell Environ 33:1935–1948

Kromdijk J, Ubierna N, Cousins AB, Griffiths H (2014) Bundle-sheath leakiness in C_4 photosynthesis: a careful balancing act between CO_2 concentration and assimilation. J Exp Bot 65:3443–3457

Kubásek J, Šetlík J, Dwyer S, Šantruc J (2007) Light and growth temperature alter carbon isotope discrimination and estimated bundle sheath leakiness in C_4 grasses and dicots. Photosynth Res 91:47–58

Meinzer FC, Zhu J (1998) Nitrogen stress reduces the efficiency of the C_4 CO_2 concentrating system, and therefore quantum yield, in Saccharum (sugarcane) species. J Exp Bot 49:1227–1234

Naidu SL, Long SP (2004) Potential mechanisms of low-temperature tolerance of C_4 photosynthesis in *Miscanthus* × *giganteus*: an in vivo analysis. Planta 220:145–155

ØBro J, Harholt J, Scheller HV, Orfila C (2004) Rhamnogalacturonan I in Solanum tuberosum tubers contains complex arabinogalactan structures. Phytochemistry 65:1429–1438

Pengelly JJ, Sirault XRR, Tazoe Y, Evans JR, Furbank RT, von Caemmerer S (2010) Growth of the C_4 dicot Flaveria bidentis: photosynthetic acclimation to low light through shifts in leaf anatomy and biochemistry. J Exp Bot 61:4109–4122

Porra RJ, Thompson WA, Kriedemann PE (1989) Determination of accurate extinction coefficients and simultaneous equations for assaying chlorophylls a and b extracted with four different solvents, verification of the concentration of chlorophyll standards by atomic absorption spectroscopy. Biochim Biophys Acta 975:384–394

Sage RF (2014) Stopping the leaks: new insights into C_4 photosynthesis at low light. Plant Cell Environ 37:1037–1041

Scheller HV, Jensen JK, Sorensen SO, Harholt J, Geshi N (2007) Biosynthesis of pectin. Physiol Plantarum 129:283–295

Sims REH, Hastings A, Schlamadinger B, Taylor G, Smith P (2006) Energy crops: current status and future prospects. Glob Change Biol 12:2054–2076

Stutz SS, Edwards GE, Cousins AB (2014) Single-cell C_4 photosynthesis: efficiency and acclimation of *Bienertia sinuspersici* to growth under low light. New Phytol 202:220–232

Sun W, Ubierna N, Ma J-Y, Cousins AB (2012) The influence of light quality on C_4 photosynthesis under steady-state conditions in *Zea mays* and *Miscanthus* × *giganteus*: changes in rates of photosynthesis but not the efficiency of the CO_2 concentrating mechanism. Plant Cell Environ 35:982–993

Sun W, Ubierna N, Ma J-Y, Walker B, Kramer D, Cousins AB (2014) The coordination of C_4 photosynthesis and the CO_2 concentrating mechanism in *Zea mays* and Miscanthus × giganteus in response to transient changes in light quality. Plant Physiol 164:1283–1292

Tazoe Y, Noguchi K, Terashima I (2006) Effects of growth light and nitrogen nutrition on the organization of the photosynthetic apparatus in leaves of a C_4 plant, *Amaranthus cruentus*. Plant Cell Environ 29:691–700

Tazoe Y, Hanba YT, Furumoto T, Noguchi K, Terashima I (2008) Relationships between quantum yield for CO_2 assimilation, activity of key enzymes and CO_2 leakiness in Amaranthus cruentus, a C_4 dicot, grown in high or low light. Plant Cell Physiol 49:19–29

Ubierna N, Sun W, Cousins AB (2011) The efficiency of C_4 photosynthesis under low light conditions: assumptions and calculations with CO_2 isotope discrimination. J Exp Bot 61:3119–3134

Ubierna N, Sun W, Kramer DM, Cousins AB (2013) The efficiency of C_4 photosynthesis under low light conditions in *Zea mays*, *Miscanthus* × *giganteus* and *Flaveria bidentis*. Plant Cell Environ 36:365–381

von Caemmerer S (2000) Biochemical models of leaf photosynthesis. CSIRO Publishing, Victoria

von Caemmerer S, Furbank RT (2003) The C_4 pathway: an efficient CO_2 pump. Photosynth Res 77:191–207

von Caemmerer S, Evans JR, Cousins AB, Badger MR, Furbank RT (2008) C_4 photosynthesis and CO_2 diffusion. In: Sheehy JE, Mitchell PL, Hardy B (eds) Charting New Pathways to C_4 Rice. International Rice Research Institue, Los Bos

von Caemmerer S, Ghannoum O, Pengelly JJ, Cousins AB (2014) Carbon isotope discrimination as a tool to explore C_4 photosynthesis. J Exp Bot 65:3459–3470

Wang D, Portis AR, Moose SP, Long SP (2008) Cool C_4 photosynthesis: pyruvate Pi dikinase expression and activity corresponds to the exceptional cold tolerance of carbon assimilation in *Miscanthus* × *giganteus*. Plant Physiol 148:557–567

Yin Z, van der Putten PEL, Driever SM, Struik PC (2016) Temperature response of bundle-sheath conductance in maize leaves. J Exp Bot. doi:10.1083/jxb/era104